Modes interaction and light transport in bidimensional organic random lasers in the weak scattering limit

M. Anni,* S. Lattante,† T. Stomeo, R. Cingolani, and G. Gigli
National Nanotechnology Laboratory (NNL) of INFM, Dipartimento di Ingegneria dell'Innovazione, Università degli Studi di Lecce, Via per Arnesano 73100 Lecce, Italy

G. Barbarella and L. Favaretto
ISOF, Area della Ricerca CNR, Via Gobetti 101, I-40129 Bologna, Italy

(Received 1 October 2003; revised manuscript received 5 August 2004; published 24 November 2004)

We report on the modes interaction and light transport in weakly scattering neat films of small molecular weight organic molecules, showing coherent random lasing. The lasing modes interaction exhibits peculiar properties, with spatially overlapped modes at low excitation density and modes competition at high excitation density. This results in a progressive decrease and in a saturation of the number of lasing modes with increasing the excitation density. The weak scattering results in diffusive light transport with a transport mean free path in the range 14.6–125 μm, which is much higher that the lasing wavelength $\lambda \approx 620$ nm. The average transport properties are correlated with the single scattering event cross section. We demonstrate that the light propagation is mainly affected by single scattering properties rather than collective effects.

DOI: 10.1103/PhysRevB.70.195216 PACS number(s): 71.55.Jv, 42.55.Zz, 42.55.Px

I. INTRODUCTION

The study of electron and light transport in disordered systems has become a prominent part of condensed matter physics. In particular the formation of bands of spatially localized electronic states, called Anderson localization, has been predicted to occur in sufficiently disordered solids,[1,2] as a consequence of the interference of electron wave functions scattered by randomly distributed defects.

Regarding light transport in disordered materials the interplay between light amplification and multiple scattering results in the fascinating phenomenon of random lasing. Such a process, after the theoretical prediction of Letokhov,[3] has recently received considerable attention, both from the fundamental point of view and for the application to microsized active elements in photonic devices.[4] Adding optical gain to a random system indeed provides a unique tool to study light transport and localization, as the behavior of lasing modes reflects the properties of the eigenstates of the disordered system.[5]

Random lasing has been demonstrated in various materials including strongly scattering tridimensional (3D) systems, like ZnO and GaN powders,[6,7] blends of TiO_2 and rhodamine dyes in solution and in inert matrix,[8,9] and weakly scattering bidimensional (2D) polymeric films.[10] Light localization has been theoretically predicted[11–17] and recently correlated to random lasing[18] for ZnO strongly scattering nanoparticles films, i.e., with the scattering mean free path length comparable to the lasing wavelength. In addition the mode interaction of the lasing modes has been investigated in strongly scattering systems, showing the occurrence of spectral and spatial modes repulsion,[9,12] as well as modes coupling.[19] In this frame, the analysis of the emission properties of random lasers in the opposite limit of weak scattering is still lacking. Some preliminary results on polymer neat films indicate a weaker scattering with respect to inorganic powders,[10,20] whereas the effects on the modes interaction of a reduced scattering efficiency, the light transport properties as well as the origin of the feedback for lasing have not been studied yet.

Moreover despite the theoretical prediction of enhancement of the localization effects as the system dimensionality is reduced,[21] most of the recent experimental works have been conducted in a strongly scattering 3D system and a detailed analysis of the emission properties of the 2D system is still missing.

In this paper we report on coherent random lasing in bidimensional (2D) neat films of low molar weight organic molecules (T5oCx, see inset of Fig. 1). We investigate the modes interaction and the light transport in asymmetric glass-T5oCx-air waveguides, which are characterized by a

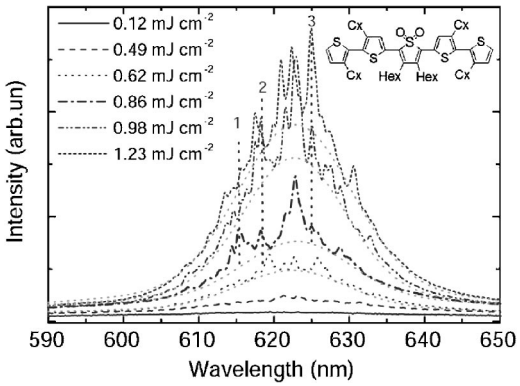

FIG. 1. Emission spectra of the S1 sample as a function of the excitation density for a stripe length of 6.5 mm. The gray lines are fit of the spectra without the contribution of random lasing peaks. The dotted vertical lines and the numbers indicate three modes with different intensity dependence on excitation density. Inset: Chemical structure of the T5oCx molecule (Hex=Hexyl chain, Cx=Ciclohexyl group).

high density of weakly scattering defects. The scattering in our system comes from morphological defects, whose scattering cross section is expected to be much smaller than that of grain boundaries in powders. Three different geometries and distributions of the scattering centers are obtained by acting on the films deposition conditions.

Despite the weak scattering coherent random lasing emission is observed in all the samples. The 2D nature of the system and the weak scattering led to modes interaction strongly different from what observed in 3D powders, due to the spatial overlap of the lasing cavities at low excitation density followed by modes repulsion only at high excitation density. This evolution is evidenced by the increase of the number of lasing modes, as the excitation density increases, followed by a decrease down to a saturation value.

We demonstrate that the light transport in the system is diffusive and we determine the transport mean free path by photoluminescence (PL) measurements as a function of the excited region length. These measurements show a critical length for lasing and a linear increase of the number of lasing modes with increasing length. The transport mean free path is in the range 14.6–125 μm for the three samples. The origin of the feedback is analyzed by atomic force microscope (AFM) measurements that show film roughness of few nanometers and cylindrical holes, acting as scattering centers, with average dimensions and distribution depending on the deposition conditions. Starting from the scattering defects geometry we analytically estimated the scattering cross section of the single scattering event and then the transport mean free path. Excellent agreement between the obtained values and the experimental ones is found, thus demonstrating that the average properties of 2D random lasers in the weak scattering regimes mainly depend on the single scattering properties rather than by collective effects.

II. EXPERIMENT

The samples were prepared by spin coating of 10^{-1}M solutions of T5oCx on glass substrates. In order to change the film morphology three different solvents have been used, namely chloroform (sample S1), dichloromethane (S2), and a 1:1 chloroform-dichloromethane blend (S3). The film thickness was about 450 nm, higher than the waveguiding cut-off, for all the samples. The excitation laser source was the third harmonic ($\lambda = 355$ nm) of a Nd-Yag laser, delivering 3 ns pulses at 1.064 μm with a repetition rate of 10 Hz. The laser was focused on the sample with a cylindrical lens, thus obtaining a 100 μm wide rectangular stripe. The length of the excited stripe was varied through a variable slit in the range 0 mm–8.5 mm. The sample emission was collected from the sample edge, dispersed by a Triax 320 mm spectrometer and detected by a Si-CCD. The spectral resolution of the measurements was about 3.5 Å. The measurements were performed at room temperature in high vacuum (about 10^{-6} mbar), in order to avoid photo-oxidation.

III. EXPERIMENTAL RESULTS

A. Effects of the excitation density

The emission spectra as a function of the excitation density for sample S1 with an excited region length of 6.5 mm are displayed in Fig. 1. For excitation density higher than about 300 $\mu J\ \mathrm{cm}^{-2}$ a 16 nm broad band due amplified spontaneous emission (ASE) appears in the spectra with a superimposed fine structure with features as narrow as 5 Å. The fine structure shows the typical behavior of coherent random lasing emission, as discussed in detail in Ref. 22.

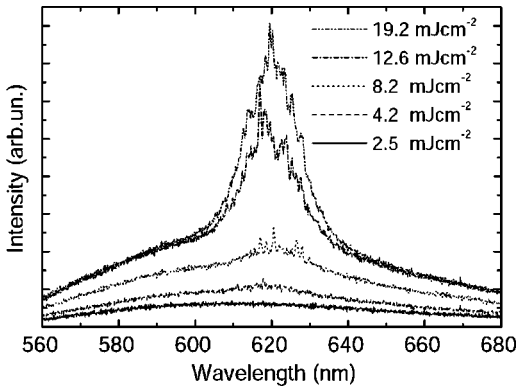

FIG. 2. Emission spectra of the S2 sample as a function of the excitation density.

The emission spectra of the S2 sample (see Fig. 2) show similar features, with an ASE band visible for excitation densities higher than 4 mJ cm^{-2} and narrow peaks due to coherent random lasing with a similar threshold. The same features are observed also for S3 samples, with an ASE and random lasing threshold of about 200 $\mu J\ \mathrm{cm}^{-2}$.

In all the investigated samples the dependence of the lasing intensity on the excitation density shows different individual behavior for different lasing modes, as shown in Fig. 3 for three different modes of the S1 spectra. In particular some of the lasing modes show an intensity increase with the excitation density typical of laser emission, as mode 3, while other modes, like mode 2, show decreasing intensity at high excitation density, and eventually disappear from the emission spectra, as mode 1.

The different dependence on the excitation density results in peculiar dependence on the excitation density of the number of lasing modes. In the spectra of all the three samples the number of lasing modes (see Figs. 4 and 5) quickly increases over threshold and reaches a maximum value for an

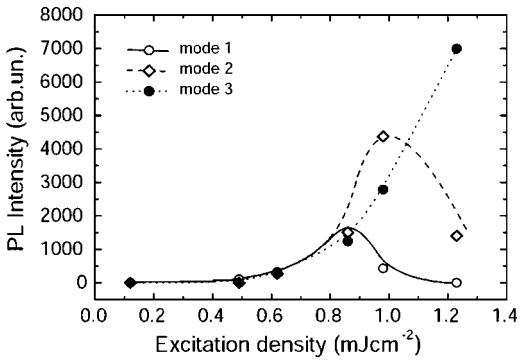

FIG. 3. Intensity of the modes 1, 2, and 3 of Fig. 1 as a function of the excitation density. The lines are guide for the eyes. The intensity decrease at high excitation density for the modes 1 and 2 is evident.

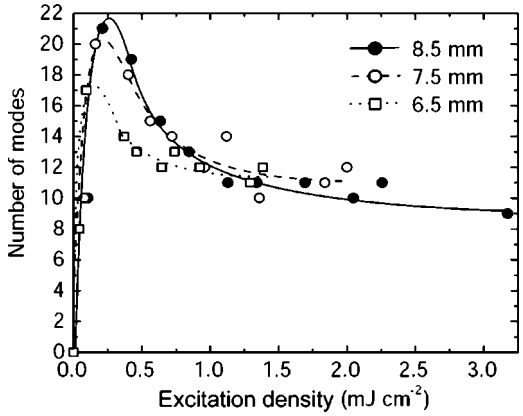

FIG. 4. Number of random lasing mode in S1 spectra as a function of the excitation density for three different stripe lengths.

excitation density about twice the lasing threshold. For higher excitation densities some of the lasing modes disappear and the total number of modes decreases down to a saturation value until the damage threshold of the film is reached.

The saturation value of the number of lasing modes has been studied for different excited stripe lengths and for different positions on the sample.

In Fig. 4 we report the number of lasing modes in sample S1 for three different excited region lengths in the same sample position of Fig. 1. The maximum number of lasing modes increases with the increase of the excited length but no significant differences can be observed at high excitation density. For shorter excited regions the saturation regime cannot be reached because the requested excitation density is higher than the damage threshold of the film. These results are quite general, regardless of the position of the excited stripe on the sample surface, even though some variations in the absolute value of the number of lasing modes from point to point may occur.

B. Effects of the system dimensions

The emission spectra of random lasing system are well known to be strongly dependent on the system dimensions.

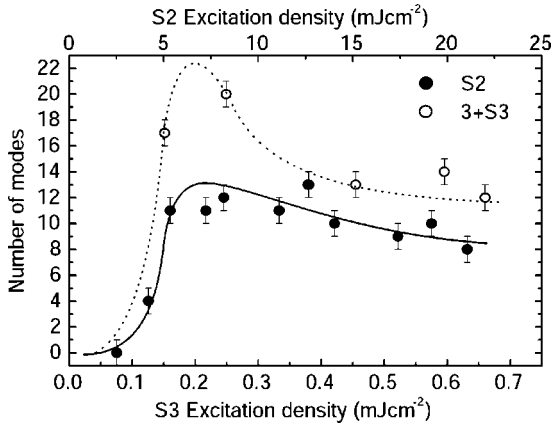

FIG. 5. Number of random lasing mode as a function of the excitation density for S2 and S3 samples. The S3 point are vertically traslated for clarity. The lines are guides for the eyes.

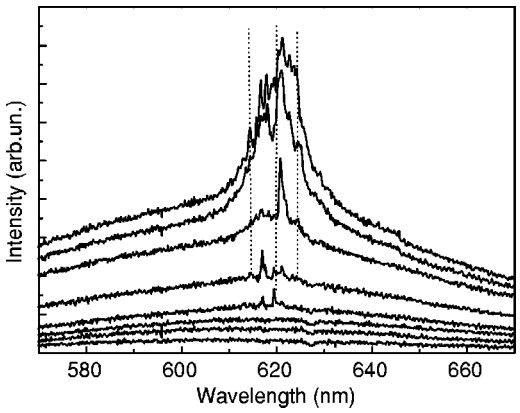

FIG. 6. Emission spectra of sample S1 as a function of the stripe length from 3.5 mm to 6.5 mm at fixed excitation density of 1.55 mJ cm^{-2}. The dotted lines indicate some modes that appear at some stripe length and persist for longer stripes.

In order to study the effects of the active system size and to have a deeper insight in the light transport in our system we performed PL measurements, at a fixed excitation density, as a function of the length of the excited region.

The emission spectra of sample S1 for an excitation density of about 1.55 mJ cm^{-2}, reported in Fig. 6, clearly show the presence of a critical length for lasing $L_{thr} \approx 4.1$ mm. When the excited region length is increased over L_{thr} an increasing number of lasing modes appears and persists as the stripe length is further increased. The dependence of the number of lasing modes on the excited stripe length (see Fig. 7) is linear over L_{thr} with a slope of about 4.6 modes/mm. The same behavior was found for the other two samples (see Fig. 7), but with some differences in the values of L_{thr} and of the slope. In the S2 sample $L_{thr} \approx 7.2$ mm and the best fit slope is slightly reduced to 4.2 modes/mm. In the S3 sample L_{thr} is reduced to 2.8 mm and the slope is increased to 7.2 modes/mm.

C. Film morphology

As in our samples we did not intentionally introduced any scattering center, it has to be expected that the scattering

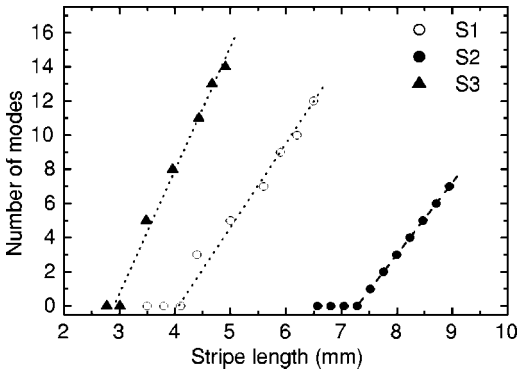

FIG. 7. Number of lasing modes as a function of the excited stripe length showing the presence of a threshold length followed by a linearly increasing number of lasing modes.

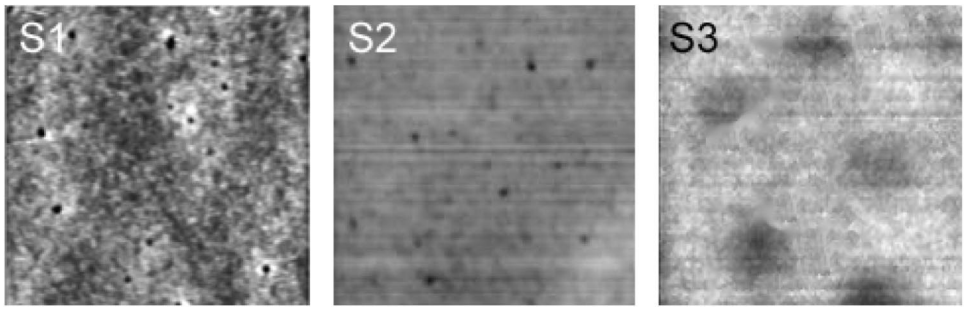

FIG. 8. 2×2 μm AFM images of the three investigated samples. The roughness is in the range 5–6 nm.

providing the feedback for random lasing comes from morphological defects. We then analyzed by atomic force microscopy (AFM) the film morphology of the three investigated samples. The AFM images of a 2.0×2.0 μm region are reported in Fig. 8.

The S1 sample shows a roughness smaller than 6 nm over several microns (see Table I), and several small holes in the film, of average radius around 25 nm, superficial defects density $N_s\approx4.0\times10^8$ cm^{-2} and a superficial defects filling factor of about 0.7%. The S2 samples shows a very similar morphology, with a roughness of about 6 nm, slightly reduces holes dimensions, but increased density. The S3 sample shows a similar roughness but with larger holes, with an average radius of about 61 nm, and reduced density.

The origin of feedback in polymers random lasers[10] was attributed to thickness fluctuations of the active films, which is expected to form random microring cavities. In our case this possibility is ruled out by the very uniform thickness. Moreover we recently demonstrated[22] that a molecule similar to T5oCx, (T5oxMe with methyl groups instead that ciclohexyl group), despite a much higher film roughness and gain values similar to T5oCx does not show coherent random lasing, but only ASE. We then conclude that in our films the feedback for lasing comes from sequential scattering from the holes in the film. Despite the high density of defects, their scattering cross section is expected to be low, as the holes are smaller than the scattered wavelength, and then weak scattering is expected.

IV. DISCUSSION

A. Effects of the excitation density: Modes interaction

The dependence of the number of lasing modes on the excitation density allows us to study the interaction between different random lasing modes in the weak scattering limit. In strongly scattering systems it has been theoretically[12] and experimentally[9] demonstrated that the number of lasing modes increases with the excitation density until it reaches a saturation value at high excitation density. Moreover the saturation value is found to linearly increase with the excited region length. These results are due to the presence of strong mode confinement, leading to non-overlapping modes. When a lasing modes reaches the lasing threshold it prevents other modes, close to its localization center and with higher losses, to reach the lasing threshold. Then only modes with far enough localization centers can lase simultaneously and a maximum number of lasing modes is observed, increasing with the system dimensions.

TABLE I. Roughness (R), holes radius (r), density (N_s), and filling factor (f) for the three investigated samples.

Sample	R (nm)	r (nm)	N_s (holes cm^{-2})	f %
S1	6	25	$4.1\cdot10^8$	0.7
S2	6	24	$5.1\cdot10^8$	0.9
S3	5	61	$1.0\cdot10^8$	1.2

Our results are instead very different, as the number of lasing modes increases up to a maximum value, but then decreases down to a saturation values at high excitation density. Moreover we observed that this results is due to the presence of some lasing modes with an intensity which decreases for high enough excitation density and disappears from the spectra. Previous studies on organic random lasers demonstrated[20] that the lasing cavities are much larger than the lasing wavelength, due to the weaker scattering, and are on average identical.

For a weakly scattering system is then reasonable to assume that partially overlapping lasing cavities are present with similar losses, and then similar lasing threshold.

We then attribute the observed trend in the number and intensity of lasing modes to the presence of spatially overlapping modes at low excitation density. When the excitation density is increased, more and more modes reach the threshold, until the mode with the highest gain prevails over the overlapping modes around its localization center. The number of modes then decreases and reaches saturation corresponding to the number of non-overlapping modes.

B. Effects of the system dimensions: Light transport

In the theory of disordered systems two very different regimes, localized and diffusive, are distinguished.[23] In the diffusive regime, for weak scattering, the eigenstates are extended and efficient light transport is possible. On the contrary, in the localization regime, requiring strong disorder, the eigenstates become localized and light transport strongly inhibited.

In order to determine the average dimensions of the lasing cavities in our system we calculated the power Fourier transform of the emission spectra over the random lasing threshold.

The typical power Fourier transform spectrum of the emission spectra (see Fig. 9) over the random lasing thresh-

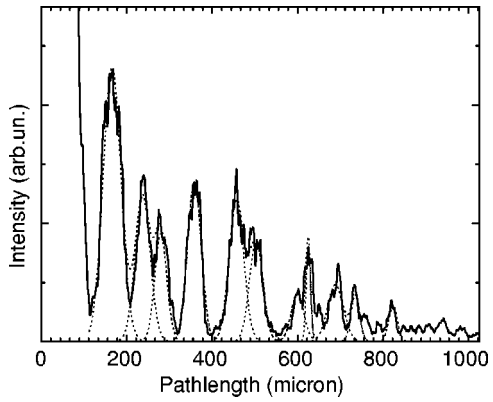

FIG. 9. Typical power Fourier transform of the S1 emission spectra over the random lasing threshold. The dotted lines represent the best fit curves of a multi-Gaussian fitting of the spectrum.

old presents clear resonances, corresponding to the length of the lasing cavities.[20] The average pathlength has been then extimated as weighted average of the peak pathlength, using their amplitudes as weights, and turned out to be about 350 μm for the S1 sample, which is much larger than the lasing wavelength, thus indicating weak scattering in the system.

In the weak scattering regime the light transport in the active medium is diffusive and can be modeled by solving by variable separation the diffusion equation with gain[3] fixing the photon flux at 0 close to the system edge. For a two-dimensional rectangular system with uniform gain and with length L_x and height L_y the lasing threshold is reached when

$$D \cdot B^2 - \frac{v}{l_g} = 0, \tag{1}$$

where $D = v l_{\mathrm{tr}}/2$ is the diffusion constant, v is the light speed in the medium, l_{tr} is the transport mean free path, $l_g = 1/g$ is the gain length and

$$B^2 = \pi^2 \cdot \left(\frac{1}{{L_x}^2} + \frac{1}{{L_y}^2} \right). \tag{2}$$

In our experiment we pump a rectangular stripe of variable length L_x and fixed height $d \approx 100$ μm. The light which is laterally scattered along the y direction leaves the excited region, with net optical gain g, and is then scattered and lost in the unexcited sample region, characterized by waveguide losses $\alpha \approx 2$ cm^{-1}. As the standard propagation length in a lossy scattering system is $\sqrt{2D/\alpha}$ we fixed $L_y \approx d + 2\sqrt{2D/\alpha}$. The g and α values for the three samples have been measured in the same excitation condition of the measurements as a function of the stripe length (Sec. III B) and are reported in Table II. The transport mean free path l_{tr} has been then determined from Eq. (1) and is reported in Table II for the three samples. In all the samples l_{tr} is much higher than the lasing wavelengths $\lambda \approx 620$ nm and much higher than the values reported for inorganic powders.[7,18]

TABLE II. Transport mean free path (l_{tr}) extracted from the threshold condition of the diffusion equation with gain. The gain value (g), the threshold stripe length (L_{thr}), and the waveguide losses (α) are also reported.

Sample	l_{tr} (μm)	g (cm^{-1})	L_{thr} (cm)	α (cm^{-1})
S1	125	2.7	0.41	2.1
S2	105	2.6	0.72	2.2
S3	14.6	2.5	0.28	2.6

C. Scattering cross section

The AFM measurements of the sample morphology suggest that the scattering defects are cylindrical holes with a defects superficial filling factor in the range 0.7%–1.2% for all the samples.

For a so low filling factor of the scattering centers the average transport properties of the disordered medium are expected to mainly depend on the scattering properties from a single defects rather than on collective effects.[24,25]

We then calculated the scattering and transport mean free paths from the scattering cross section per unitary length σ' of a single defect. The exact cross section for scattering of a plane wave of wavelength λ from a finite cylinder of radius r and length L can be easily performed[26] in the limits of very small cylinders, i.e., $r, L \ll \lambda$ (Rayleigh scattering), and in the opposite limit of very long thin cylinders, i.e., $r \ll \lambda$ and $L \gg \lambda$. In our case, as L is comparable with λ and the aspect ratio is between 5 and 9, the cross section for a plane wave cannot be trivially extimated and numerical techniques are necessary.[27–31] However in our experiment we studied the light propagation in a 2D disordered asymmetric waveguides air-organic-glass, so we are not dealing with a plane wave, but with the TE (electric field in the plane of the waveguide) guided mode. The electric field amplitude is then maximum close to the waveguides center and vanishing close to the interfaces. Moreover it's known[30] that in the central region of a finite cylinder the elements of the polarization matrix are very close to the values of infinite cylinders already for an aspect ratio of 5. We then estimated σ' by using the values for an infinite cylinder perpendicular to the light propagation direction and for TE polarization (electric field perpendicular to the cylinder axes). As the scattering mainly occurs in a plane perpendicular to the cylinder axes[26] it is also reasonable to assume that all the scattered light continues to propagate in the guide plane, so that the total scattering cross section can be used. For very thin cylinder the total scattering and transport cross section are then given by[26]

$$\sigma'_{\mathrm{sca}} = \frac{2}{\pi k} \int_0^{2\pi} |T(\theta)|^2 d\theta = \frac{4}{k} \left(\frac{\pi x^2}{4} \right)^2 (n^2 - 1)^2 \times \left[\frac{x^4}{64} + \frac{2}{(n^2+1)^2} \right], \tag{3}$$

TABLE III. Scattering and transport cross section and mean free path extracted from the defects geometry and distribution of the three investigated samples.

Sample	σ'_{sca} (cm)	σ'_{tr} (cm)	l_{sca} (μm)	l_{tr} (μm)
S1	$2.37\cdot10^{-7}$	$2.37\cdot10^{-7}$	105	105
S2	$2.01\cdot10^{-7}$	$2.01\cdot10^{-7}$	97.7	97.7
S3	$8.18\cdot10^{-6}$	$8.16\cdot10^{-6}$	12.2	12.3

$$\sigma'_{tr} = \frac{2}{\pi k}\int_0^{2\pi} |T(\theta)|^2(1-\cos\theta)d\theta = \sigma'_{sca} - \frac{1}{k}\left(\frac{\pi^2 x^6}{64}\right)\frac{(n^2-1)^2}{(n^2+1)^2}, \tag{4}$$

where k is the wave number, $x=k\cdot r$, θ is the scattering angle in the propagation plane, and n is the organic refractive index. The relation between σ'_{sca} and σ'_{tr} in the low concentration limit[25] is $\sigma'_{sca}\cdot l_{sca}=\sigma'_{tr}\cdot l_{tr}$. By substituting the values for k, r, and $n=1.8$ (determined from reflectance and transmittance measurements) we obtain σ'_{sca} and σ'_{tr}, the values are reported in Table III.

In order to extract the transport and scattering mean free paths from the corresponding cross section, and to compare them with the experimental values, it is very important to know the degree of order of the defects distribution. In particular the presence of spatial correlation in the defects position is known to strongly influence the emission properties of random lasers in the diffusive regime.[16,32] Moreover, as the holes providing the feedback for lasing are formed during the spin coating process, correlation effects similar to the ones observed in organic droplets grown by evaporation could be present.[33]

We then estimated for all the samples the height-height correlation function defined as

$$g(r) = \langle [h(\mathbf{r}_1) - h(\mathbf{r}_2)]^2 \rangle, \tag{5}$$

where $\mathbf{r}_1$ and $\mathbf{r}_2$ are the position vector of two generic points in the sample at distance r and the brackets indicate the averaging over all the sample surface. The obtained curves, reported in Fig. 10, show a regular increase with r and a saturation for r higher than about 1 micron, but no evident peaks, denoting correlation, are present. We then conclude that the defects distribution is random in all the investigated samples.

The scattering and transport mean free paths have been then determined through the relations $1/l=\sigma' N_s$. The obtained values, reported in Table III are in excellent agreement with the experimental values extracted from the diffusion equation with gain (Fig. 11), thus indicating that the average transport properties in our samples are mainly influenced by the single scattering properties and not by collective effects.

V. CONCLUSIONS

In conclusion we reported on modes interaction and light transport in weakly scattering 2D organic films showing coherent random lasing even in the diffusive regime. The weak scattering results in a peculiar modes interaction, with spatial mode overlap at low excitation density and mode competition and suppression at high excitation density. The light transport in the samples is diffusive with a transport mean free path in the range 14.6–125 μm, much higher than the lasing wavelength $\approx$620 nm. The average transport properties have been then correlated with the scattering cross section of a single scattering defects, of geometry and distribution obtained from AFM measurements. The theoretical scattering and transport mean free path are in excellent agreement with the experimental ones, demonstrating that the light propagation in our system is mainly influenced by single scatterer properties rather than by collective processes.

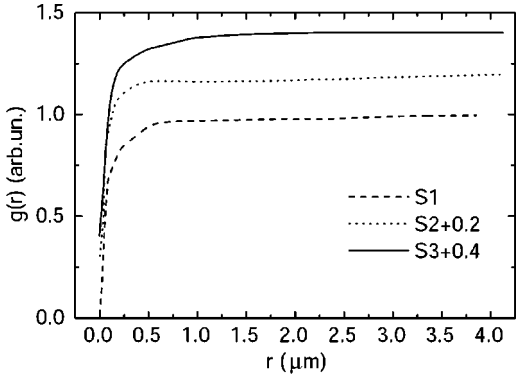

FIG. 10. Height correlation function of the three samples. The curves are normalized to their saturation value and vertically translated for clarity.

ACKNOWLEDGMENTS

The authors would like to acknowledge Roberto Rella and Francesca Chetta for the refractive index determination, Mauro Lomascolo and Massimo De Vittorio are acknowledged for useful discussions. One of the authors (M.A.) particularly acknowledges Raimondo Anni for continuous teachings and stimulating discussions.

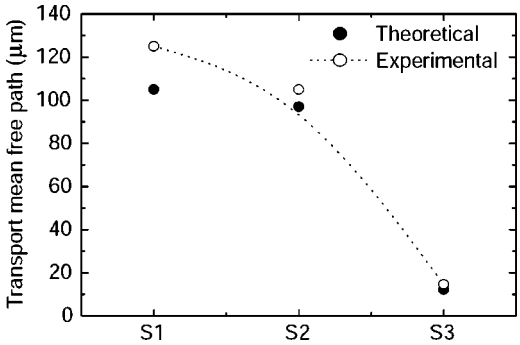

FIG. 11. Transport mean free path obtained from the calculated cross section (full dots) compared with the values obtained from the diffusion equation (empty dots). The good agreement is evident.

*Electronic address: marco.anni@unile.it
†Also at Dipartimento di Fisica, Universitá degli Studi di Lecce, Via per Arnesano 73100 Lecce, Italy

[1] P. W. Anderson, Phys. Rev. **109**, 1492 (1958).
[2] P. W. Anderson, Rev. Mod. Phys. **50**, 191 (1978).
[3] V. S. Lethokov, Sov. Phys. JETP **26**, 835 (1968).
[4] D. Wiersma, Nature (London) **406**, 132 (2000).
[5] X. Jiang and C. M. Soukoulis, Phys. Rev. E **65**, 025601 (2002).
[6] H. Cao, Y. G. Zhao, H. C. Ong, S. T. Ho, J. Y. Dai, J. Y. Wu, and R. P. H. Chang, Appl. Phys. Lett. **73**, 3656 (1998).
[7] H. Cao, Y. G. Zhao, S. T. Ho, E. W. Seelig, Q. H. Wang, and R. P. H. Chang, Phys. Rev. Lett. **82**, 2278 (1999).
[8] H. Cao, J. Y. Xu, S. H. Chang, and S. T. Ho, Phys. Rev. E **61**, 1985 (2000).
[9] Y. Ling, H. Cao, A. L. Burin, M. A. Ratner, X. Liu, and R. P. H. Chang, Phys. Rev. A **64**, 063808 (2001).
[10] S. V. Frolov, Z. V. Vardeny, K. Yoshino, A. Zakhidov, and R. H. Baughman, Phys. Rev. B **59**, R5284 (1999).
[11] Z. Q. Zhang, Phys. Rev. B **52**, 7960 (1995).
[12] X. Jiang and C. M. Soukoulis, Phys. Rev. Lett. **85**, 70 (2000).
[13] M. Rusek and A. Orlowski, Phys. Rev. E **59**, 3655 (1999).
[14] M. M. Sigalas, C. M. Soukoulis, C. T. Chan, and D. Turner, Phys. Rev. B **53**, 8340 (1996).
[15] P. Sebbah and C. Vanneste, Phys. Rev. B **66**, 144202 (2002).
[16] V. M. Apalkov, M. E. Raikh, and B. Shapiro, Phys. Rev. Lett. **89**, 016802 (2002).
[17] C. Vanneste and P. Sebbah, Phys. Rev. Lett. **87**, 183903 (2001).
[18] H. Cao, J. Y. Xu, D. Z. Zhang, S. H. Chang, S. T. Ho, E. W. Seelig, X. Liu, and R. P. H. Chang, Phys. Rev. Lett. **84**, 5584 (2000).
[19] H. Cao, X. Jiang, Y. Ling, J. Y. Xu, and C. M. Soukoulis, Phys. Rev. B **67**, 161101(R) (2003).
[20] R. C. Polson, M. E. Raikh, and Z. V. Vardeny, Physica E (Amsterdam) **13**, 1240 (2002).
[21] S. John, Phys. Rev. Lett. **53**, 2169 (1984).
[22] M. Anni, S. Lattante, R. Cingolani, G. Gigli, G. Barbarella, and L. Favaretto, Appl. Phys. Lett. **83**, 2754 (2003).
[23] C. W. J. Beenakker, Rev. Mod. Phys. **69**, 731 (1997).
[24] M. P. van Albada, B. A. van Tiggelen, A. Lagendijk, and A. Tip, Phys. Rev. Lett. **66**, 3132 (1991).
[25] K. Busch, C. M. Soukoulis, and E. N. Economou, Phys. Rev. B **50**, 93 (1994).
[26] H. C. van de Hulst, *Light Scattering by Small Particles* (Dover, New York, 1981).
[27] N. K. Uzunoglu, N. G. Alexopulos, and J. G. Fikioris, J. Opt. Soc. Am. **68**, 194 (1978).
[28] L. D. Cohen, R. D. Haracz, and A. Cohen, Appl. Opt. **22**, 742 (1983).
[29] J. W. Shepherd and A. R. Holt, J. Phys. A **16**, 651 (1983).
[30] R. D. Haracz, L. D. Cohen, and A. Cohen, Appl. Opt. **23**, 436 (1984).
[31] F. Kuik, J. F. de Haan, and J. W. Hovenier, Appl. Opt. **33**, 4906 (1994).
[32] M. Patra, Phys. Rev. E **67**, 065603 (2003).
[33] M. Brinkmann, F. Biscarini, C. Taliani, I. Aiello, and M. Ghedini, Phys. Rev. B **61**, R16339 (2000).